Structural and Kinetic Studies of Spin Crossover in an Iron(II) Complex with a Novel Tripodal Ligand

Ala H. R. Al-Obaidi,[†] Kenneth B. Jensen,[‡] John J. McGarvey,*[,†] Hans Toftlund,*[,‡] Bent Jensen,[‡] Steven E. J. Bell,*[,†] and Jonathan G. Carroll[†]

School of Chemistry, Queen's University of Belfast, Belfast BT9 5AG, Northern Ireland, and Department Of Chemistry, Odense University, Odense, DK 5230, Denmark

Received February 29, 1996[⊗]

Configurational and ligand conformational influences on the kinetics of $^1A_1 \rightleftharpoons {}^5T_2$ spin crossover in the Fe(II) complex with the novel tripodal ligand, 1,1,1-tris((*N*-(2-pyridylmethyl)-*N*-methylamino)methyl)ethane (tptMetame), have been explored. Despite having six chelate rings and three chiral nitrogen atoms, only one enantiomeric pair of isomers, Δ, *SSS*, and Λ, *RRR*, of the complex ion is observed. The conformation of the three rings forming the upper "cap" of the complex structure can be assigned δ or λ with respect to the 3-fold molecular axis. X-ray data at 300 and 153 K, above and below the critical temperature for the spin transition, show that the conformation of the ligand "cap" is the same as the absolute configuration of the complex, with the same $\Lambda\lambda^{CAP}$(or $\Delta\delta^{CAP}$) combination prevailing for both the LS ($^1A_1$) and HS ($^5T_2$) isomers. Molecular mechanics calculations further show that the ligand energy remains lowest for this $\Lambda\lambda^{CAP}$ (or $\Delta\delta^{CAP}$) combination at all Fe−N distances over the range spanning the LS and HS isomers. Measurements of the spin crossover relaxation time have been carried out in solution over the temperature range 293−170 K. The observed monophasic relaxation traces are also consistent with the absolute configuration of the complex remaining unaltered during the spin crossover.

Introduction

Spin crossover in iron complexes has been extensively studied in both solution and in the solid state. The subject has recently been comprehensively reviewed.[1] Several of the recent studies in solution have involved the strategy of using ligand design to control the lifetimes of the spin isomers.[2,3] Among the examples are cases in which the spin state relaxation following laser photoperturbation is marked by a biphasic decay,[2,4] coupling of molecular conformational changes to metal−ligand bond length changes in the complex being proposed as an explanation.[2]

We report here an example of a complex involving a novel tripodal ligand where the stereochemistry dictates that the same enantiomer prevails for both the low- and high-spin forms. X-ray crystallographic data are presented for the complex and molecular mechanics calculations have been used to supplement the structural data. The relaxation kinetics of the spin crossover in solution following pulsed laser photoperturbation has been investigated over a wide temperature range.

Experimental Section

Synthesis. 1,1,1-Tris((methylamino)methyl)ethane (tMetame) was prepared from 1,1,1-tris(bromomethyl)ethane after the method of Kasowski and Bailar.[5] Yield: 57%.

^{1}H NMR (in $CDCl_3$), ppm: 2.5, singlet (6H) CH_2; 2.4, singlet (9H) N−CH_3; 1.3, singlet (3H) NH; 0.9, singlet (3H) C−CH_3.

1,1,1-Tris((*N*-(2-pyridylmethyl)-*N*-methylamino)methyl)ethane (tptMetame). 2-Pyridylmethyl chloride hydrochloride (6.2 g, 37.7 mmol) in water (50 mL) was slowly added to a mixture of sodium hydroxide (4 g, 100 mmol) in water (100 mL) and 1,1,1-tris(methylaminomethyl)-ethane (2 g, 12.6 mmol) in methylene chloride (50 mL). The mixture was stirred vigorously for 72 h. The aqueous phase was extracted three times with methylene chloride (150 mL) and the combined organic phases were dried over magnesium sulfate. Evaporation in vacuum yielded an orange oily product (35%). The crude product was purified via complex formation (see below) with nickel(II) perchlorate, recrystallization, and liberation of the ligand with sodium cyanide. ^{1}H NMR (in $CDCl_3$), ppm: 7.0−8.6, multiplet (12H) py; 3.7, singlet (6H) CH_2−py; 2.5, singlet (6H) CH_2−N; 2.3, singlet (9H) N−CH_3; 1.1, singlet (3H) C−CH_3.

Warning! The following complexes, isolated as the perchlorate salts, were treated as potentially explosive.

1,1,1-Tris((*N*-(2-pyridylmethyl)-*N*-methylamino)methyl)ethane)-nickel(II) Perchlorate ([Ni(tptMetame)](ClO$_4$)$_2$). Crude 1,1,1-tris-((*N*-(2-pyridylmethyl))-*N*-methylamino)methyl)ethane (0.5 g 1.2 mmol) in ethanol (10 mL) was added to nickel(II) perchlorate (0.42 g, 1.2 mmol) in ethanol (10 mL) with stirring. The pink precipitate was isolated and recrystallized from a 1:1 mixture of acetone and water. Yield: 0.72 g (90%).

Anal. Calcd for Ni $C_{26}H_{36}N_6O_8Cl_2$, H_2O: C, 44.10; H, 5.40; N, 11.87; Cl, 10.01. Found: C, 44.60; H, 5.11; N, 11.88; Cl, 9.80.

UV−vis in acetonitrile (λ/nm (ϵ/M^{-1} cm^{-1})): 312 (303, sh); 543 (15); 812 (9, sh); 872 (10).

1,1,1-Tris((*N*-(2-pyridylmethyl)-*N*-methylamino)methyl)ethane iron(II) Perchlorate [Fe(tptMetame)](ClO$_4$)$_2$). This preparation was carried out in a nitrogen atmosphere. Pure 1,1,1-tris((*N*-(2-pyridyl-methyl)-*N*-methylamino)methyl)ethane (0.9 g, 2.1 mmol) was added to iron(II) perchlorate (0.76 g, 2.1 mmol) in a 1:1 mixture of methanol and water (20 mL) preheated to 50 °C. When the mixture was cooled to room temperature, a light green precipitate was formed. Yield: 1.1 g (78%).

Anal. Calcd for Fe $C_{26}H_{36}N_6O_8Cl_2$: C, 45.43; H, 5.28; N, 12.23; Cl, 10.32. Found: C, 45.38; H, 5.34; N, 11.96; Cl, 10.05.

Crystals suitable for X-ray measurements were obtained by recrystallization from acetonitrile.

Physical Techniques. The laser photoperturbation method[6] has been described previously.[7] The irradiation source was a Q-switched Nd/

[†] Queen's University of Belfast.
[‡] Odense University.
[⊗] Abstract published in *Advance ACS Abstracts,* July 15, 1996.
(1) Gütlich, P.; Hauser, A.; Spiering, H. *Angew. Chem., Int. Ed. Engl.* **1994**, *33*, 2024.
(2) Al-Obaidi, A. H. R.; McGarvey, J. J.; Taylor, K. P.; Bell, S. E. J.; Jensen, K. B.; Toftlund, H. *J. Chem. Soc. Chem. Commun.* **1993**, 536.
(3) Toftlund, H. *Spin-Ligevaegt i Jern(II) Komplekser;* Trykt hos Mamen: Odense, Denmark, **1987**.
(4) McCusker, J. K.; Toftlund, H.; Rheingold, A. L.; Hendrickson, D. N. *J. Am. Chem. Soc.* **1993**, *115*, 1797.
(5) Kasowski, W. J.; Bailar, J. C. *J. Am. Chem. Soc.* **1963**, *91*, 3212.

S0020-1669(96)00228-5 CCC: $12.00

Table 1. Crystallographic Data and Details of Data Collection and Structure Analyses for [Fe(tptMetame)]$(ClO_4)_2$ at 153 K

formula	$C_{26}H_{36}N_6O_8Cl_2Fe$	T, K	153
fw, g/mol	687.4	λ(Mo Kα), Å	0.710 73
cryst dimens, mm	0.3 × 0.2 × 0.2	ρ_{calc}, g cm^{-3}	1.535
space group	$P2_1/n$	μ(Mo Kα), cm^{-1}	7.4
a, Å	10.141(13)	no. of indep reflcns	4019
b, Å	21.132(6)	no. of variables	496
c, Å	13.895(8)	F(000)	4019
β, deg	92.70(7)	R[a]	0.059
V, Å^3	2974.5	R_w[b]	0.059
Z	4		

[a] $R = \sum||F_o| - |F_c||/\sum|F_o|$. [b] $R_w = [\sum w(|F_o| - |F_c|)^2/\sum w|F_o|^2]^{1/2}$.

YAG laser coupled to either a dye laser or a Raman wavelength-shifting cell to provide a range of excitation wavelengths. Typical pulse energy and width were *ca* 10 mJ and 8−9 ns respectively. The excitation laser beam was unfocused and the irradiated sample area was *ca*. 0.4 cm^2. Transient changes in sample absorbance following pulsed irradiation were detected by means of a rapid response spectrophotometric system with a boosted xenon arc monitoring source. Solutions (*ca*. 10^{-3} mol dm^{-3}) in *n*-propionitrile or *n*-butyronitrile or in 4:5 (v/v) mixtures of these two solvents were prepared *in vacuo* by distilling the degassed solvent onto the solid sample contained in a 1 cm fluorimeter cell. The sealed cell was placed in a polystyrene block and the sample temperature (±1 °C) could be varied over the range 300−170 K by flowing cooled N_2 gas through channels cut into the block.

UV−vis measurements were made using a HP 8452A diode array spectrometer. A similar arrangement was used to control the sample cell temperature as for the pulsed laser relaxation measurements.

Single-crystal X-ray diffraction was carried out using an Enraf-Nonius CAD-4 diffractometer. The intensity data were corrected for Lorentz and polarization effects and for absorption. The structure was solved by the direct method (SHELXS-86)[8] and refined by the full-matrix least-squares method (SHELX-76).[9] Details of X-ray structural data collection are given in Table 1.

Magnetic moment measurements were made with equipment described elsewhere.[10] Molecular mechanics calculations were run on a PC using the MM+ forcefield within the Hyperchem molecular modeling package.[11] Geometry optimization was carried out at a series of constrained Fe−N distances. For each of these optimized geometries, the single point energy for the ligand alone was then calculated.

Results and Discussion

Molecular and Crystal Structure of [Fe(tptMetame)]$(ClO_4)_2$. This complex crystallizes in the monoclinic space group $P2_1/n$. The structure was solved at 153 K and a preliminary structure at 300 K is available and will be referred to in the discussion below. There are four complex cations in the unit cell, in sets of two enantiomeric pairs. Figure 1 shows a drawing of the cation and the numbering scheme employed. Atomic coordinates are given in Table 2. Selected bond distances and angles are given in Table 3. A full data set is available in the supplementary material.

It is apparent from Figure 1 that tptMetame acts as a hexadentate ligand. The weighted mean Fe−N(py) and Fe−N(aliphatic) distances are 2.21(3) and 2.26(3) Å respectively at 300 K. These distances change to 1.993(3) and 2.093(3) Å on cooling to 153 K, where the complex is predominantly low spin.

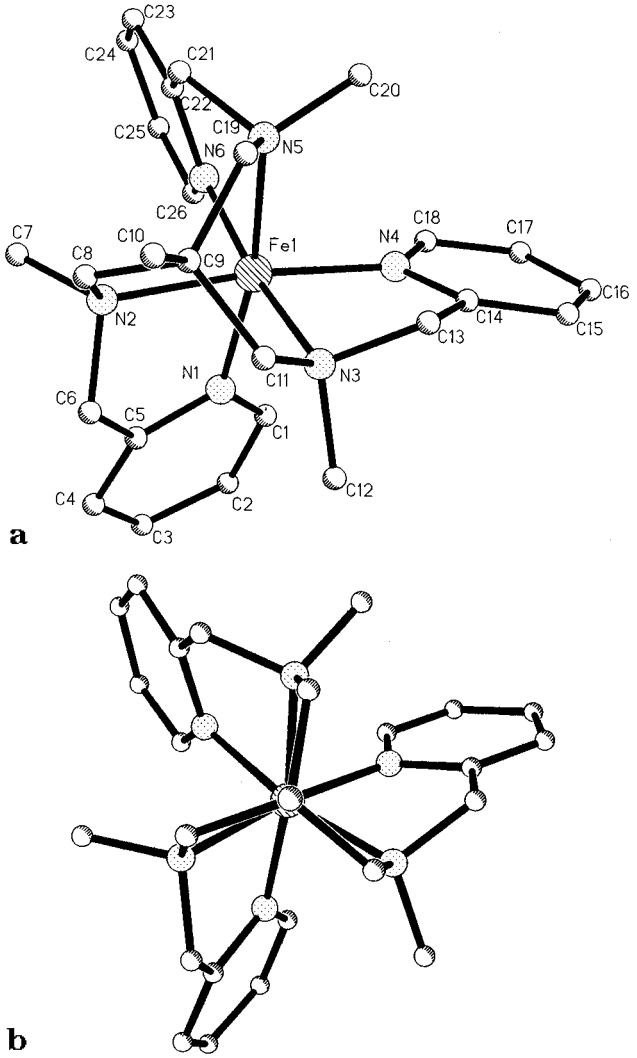

Figure 1. (a) Drawing of the [Fe(tptMetame)]$^{2+}$ cation, showing the numbering scheme. (b) view down the C_3 axis.

The bond length changes between the low-temperature and the high-temperature structures are $\Delta r = 0.21$ and 0.16 Å for the Fe−N(py) and Fe−N(aliphatic) distances respectively, comparable to what have been observed for other similar systems.[12] However, in comparison to the $[Fe(pic)_3]Cl_2$·ethanol(pic = (2-pyridylmethyl)amine) system,[13] the present complex shows a 12% lower change in the Fe−N(aliphatic) distances. This is likely to be the result of the increased steric restrictions of the present ligand. It is anticipated that fusing three five-membered pyridylmethyl chelate rings to the tripodal 1,1,1-tris(aminomethyl)amine unit in the present ligand would result in a rather inflexible molecule. An important parameter in the discussion of the geometry of hexadentate tripodal ligands is the twist angle ϕ between the two opposite trigonal faces along the 3-fold axis. This angle can vary from zero for a trigonal prismatic complex to 60° for an octahedral complex. In the present case ϕ values of 45.5° and 51.0° at 300 and 153 K, respectively, were determined on the basis of the X-ray data. Although the lower value is observed for the high-spin form, which has the lower ligand-field preference for an octahedral geometry, the actual change in ϕ in going from high-spin to low-spin is small, which again reflects the stiffness of the ligand. As expected, the largest geometrical changes accompanying the spin change are the distances between the donor atoms along the edges not bridged

(6) McGarvey, J. J.; Lawthers, I. *J. Chem. Soc., Chem. Commun.* **1982**, 906.
(7) McGarvey, J. J.; Toftlund,H.; Al-Obaidi, A. H. R.; Taylor, K. P.; Bell, S. E. J. *Inorg. Chem.* **1993**, *32*, 2469.
(8) Sheldrick, G. M. *Program for Solution of Crystal Structure*; University of Göttingen: Göttingen, Germany.
(9) Sheldrick, G. M. *Program for Solution of Crystal Structure*; University of Cambridge: Cambridge, England.
(10) Josephsen, J.; Pedersen, E. *Inorg. Chem.* **1977**, *16*, 2534.
(11) Hyperchem. Release 3, **1992**, for Windows. Autodesk, Inc. 2320 Marinship Way Sausalito, CA.
(12) Toftlund, H. *Coord. Chem. Rev.* **1989**, *94*, 67.
(13) Mikami, M.; Konno, M.; Saito, Y. *Chem Phys Lett.*, **1979**, *63*, 566.

Table 2. Atomic Coordinates and Isotropic Thermal Parameters (Å^2) for [FetptMetame](C10$_4$)$_2$ Omitting the Anions and H Atoms at 153 K

atom	*X*/*a*	*Y*/*b*	*Z*/*c*	*U*(iso)/*U*(eq)
Fel	0.5022(1)	−0.1500(0)	0.3452(0)	0.0222(2)
N1	0.3822(4)	−0.2250(2)	0.3505(3)	0.028(1)
N2	0.6486(4)	−0.2208(2)	0.3578(3)	0.028(1)
N3	0.5046(4)	−0.1514(2)	0.1950(3)	0.029(1)
N4	0.3551(4)	−0.0887(2)	0.3177(3)	0.027(1)
N5	0.6470(4)	−0.0801(2)	0.3550(3)	0.025(1)
N6	0.5064(4)	−0.1381(2)	0.4864(3)	0.024(1)
C1	0.2535(6)	−0.2262(3)	0.3695(4)	0.035(2)
C2	0.1856(6)	−0.2816(3)	0.3874(4)	0.041(2)
C3	0.2515(6)	−0.3384(3)	0.3856(4)	0.041(2)
C4	0.3830(6)	−0.3380(3)	0.3634(4)	0.040(2)
C5	0.4434(6)	−0.2812(2)	0.3439(4)	0.030(2)
C6	0.5813(6)	−0.2770(2)	0.3133(4)	0.033(2)
C7	0.6909(6)	−0.2439(2)	0.4572(4)	0.035(2)
C8	0.7672(5)	−0.2056(3)	0.3052(4)	0.033(2)
C9	0.7543(5)	−0.1513(3)	0.2310(4)	0.032(2)
C10	0.8785(6)	−0.1519(3)	0.1731(4)	0.044(2)
C11	0.6384(6)	−0.1617(2)	0.1585(4)	0.033(2)
C12	0.4090(6)	−0.1955(3)	0.1431(4)	0.038(2)
C13	0.4559(6)	−0.0866(3)	0.1669(4)	0.034(2)
C14	0.3462(5)	−0.0684(2)	0.2253(4)	0.029(2)
C15	0.2376(6)	−0.0321(3)	0.1912(4)	0.033(2)
C16	0.1437(5)	−0.0155(3)	0.2517(4)	0.034(2)
C17	0.1537(5)	−0.0341(2)	0.3474(4)	0.031(2)
C18	0.2621(5)	−0.0700(2)	0.3766(4)	0.027(2)
C19	0.7478(5)	−0.0861(2)	0.2801(4)	0.030(2)
C20	0.6007(5)	−0.0134(2)	0.3560(4)	0.027(2)
C21	0.7127(5)	−0.0896(2)	0.4520(4)	0.026(1)
C22	0.6167(5)	−0.1081(2)	0.5228(3)	0.023(1)
C23	0.6370(5)	−0.0986(2)	0.6218(4)	0.027(1)
C24	0.5454(5)	−0.1189(2)	0.6835(4)	0.029(2)
C25	0.4325(5)	−0.1487(2)	0.6464(4)	0.030(2)
C26	0.4195(5)	−0.1579(2)	0.5487(4)	0.027(1)

Table 3. Selected Bond Lengths (Å) and Angles (deg) for Fe(tptMetame)](ClO$_4$)$_2$ at 153 K

	Bond Lengths		
Fe−N1	2.002(4)	Fe−N(4)	2.000(4)
Fe−N2	2.108(4)	Fe−N(5)	2.083(4)
Fe−N3	2.088(4)	Fe−N(6)	1.978(4)
	Bond Angles		
N1−Fe−N2	82.1(2)	N2−Fe−N6	91.5(2)
N1−Fe−N3	93.5(2)	N3−Fe−N4	82.1(2)
N1−Fe−N4	94.1(2)	N3−Fe−N5	91.9(2)
N1−Fe−N5	170.8(2)	N3−Fe−N6	173.2(2)
N1−Fe−N6	92.8(2)	N4−Fe−N5	94.0(2)
N2−Fe−N3	91.8(2)	N4−Fe−N6	95.1(2)
N2−Fe−N4	172.6(2)	N5−Fe−N6	82.1(2)
N2−Fe−N5	90.4(2)		

by chelates (N1−N4, N4−N6, N1−N6, Figure 1). The mean of these distances increases from 2.915(3) to 3.32(3) Å, on heating from 153 to 300 K.

Stereochemistry. The complex cation has six chelate rings and three chiral nitrogen donor atoms, potentially giving rise to a large number of isomers. The three six-membered chelate rings spanning the aliphatic nitrogen donors share and are constrained by the sp^3-hybridized bridgehead carbon atom to adopt the same conformations exclusively. The conformation of the three rings in the upper "cap" of the ligand can thus be assigned collectively as δ^{CAP}or $\lambda^{CAP}$with respect to the 3-fold axis.[14] The three five-membered pyridyl amine chelates also can adopt δ or λ conformations, but their conformations are linked via the amine nitrogen donors to the conformations of the six-membered chelate rings in the cap. In the X-ray structure they adopt the opposite conformation to the conformation of the cap. Dreiding molecular models clearly indicate that isomers with different chirality around the three aliphatic nitrogens are sterically hindered, suggesting an explanation for the fact that only isomers with C_3 molecular symmetry are observed. As the direction of a given pyridyl amine chelate is linked to the chiral nitrogen atom this chirality also dictates the absolute configuration of the complex. The Δ and Λ configurations are associated with *S* and *R* chirality of the three aliphatic nitrogens respectively, so that only the Δ,*SSS* and Λ,*RRR* enantiomeric pair is possible. For the Fe(II) complex under investigation here, since inversion around the chiral N atom cannot occur unless all the Fe−N bonds are broken it is clear that configurational inversion has a very high barrier.[15] In the X-ray structure the "conformation" of the cap is the same as the absolute configuration of the complex. The enantiomeric pair in the crystal structure is therefore fully described by the designations $\Lambda\lambda^{CAP}\delta\delta\delta$ / $\Delta\delta^{CAP}\lambda\lambda\lambda$. The same enantiomeric pair is observed for the high spin form of the complex, a result intimated by molecular mechanics calculations. The latter show that diastereomers where the conformation of the cap is opposite to the absolute configuration or where the conformation of the cap is the same as that of the pyridyl methyl chelates both have higher ligand strain energy than the isomer actually observed, *(see below)*.

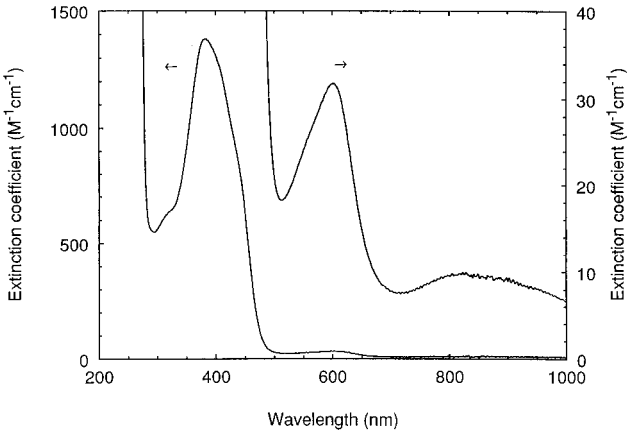

Figure 2. Electronic spectrum of [Fe(tptMetame)](ClO$_4$)$_2$ in acetonitrile. At room temperature the low-spin fraction is approximately 15%.

Electronic Spectra. The room temperature electronic spectrum of [Fe(tptMetame)]$^{2+}$ in acetonitrile is shown in Figure 2. A striking feature of the present complex is its green color. This is in contrast to other spin-crossover systems with a similar combination of amine and imine nitrogen donors which are normally red. The reason for this unexpected color is a large red shift and increased intensity of the first ligand field band $^1T_1 \leftarrow {}^1A_1$, combined with the blue-shifted and low intensity charge-transfer bands at room temperature. For iron(II) complexes of imine-containing ligands, the first low-spin ligand field band is in general masked by the MLCT transition. However, in the present case this band is clearly resolved at 601 nm. A low value of the ligand field splitting parameter, Δ_{LS}, which this band position indicates, is consistent with the rather long average Fe−N distances found for this structure. The crystal field model predicts that Δ is inversely proportional to the sixth power of the metal−ligand distance. The average Fe−N distance for the present complex is 0.03 Å longer than

(14) Assigning the conformation of the cap with respect to the C_3 axis as δ in the present case is equivalent to all three chelate rings having the λ conformation, and *vice versa.*

(15) The ^{1}H NMR spectra of the Co(III) and Zn(II) complexes show a doublet of doublets pattern in the CH$_2$ regions. Thus the two hydrogens at each carbon experience different environments even in the zinc complex. This result indicates that the configurational inversion is slow on the NMR time scale for both complexes.

for the $[Fe(tp(10)aneN_3)](ClO_4)_2$ complex[16] (which has a very similar donor set), where the first ligand field band is observed as a shoulder around 570 nm.[17] Assuming the energy of the first band varies linearly with Δ_{LS}, this predicts a position around 626 nm, even lower than that actually observed.

The ligand field transition $^5E \leftarrow {}^5T_2$ of the high-spin Fe(II) species is observed as a broad and weak feature around 820 nm corresponding to a Δ_{HS} value of 12 200 cm^{-1}, which is typical for these types of complexes. As the Δ_{HS} values for Fe(II) high spin complexes are generally found to be some 5% higher than for the corresponding nickel complexes,[18] this is consistent with the Δ value for the $[Ni(tptMetame)]^{2+}$ complex, which is 11 573 cm^{-1}. This value is obtained after analysing the low energy band in the spectrum of $[Ni(tptMetame)]^{2+}$ with the assumption that the appearance of the band is caused by mixing of the first singlet state,[1]E, into the $^3T_2$ state.[19]

In order to estimate the thermodynamic parameters in solution for the spin crossover process, absorption spectra of $[Fe(tptMetame)]^{2+}$ in propionitrile (*ca.* 10^{-3} mol dm^{-3}) were recorded at 10 different temperatures over the range 203−295 K. The spectra were analyzed on the assumption that $\Delta H°$ and $\Delta S°$ are temperature-independent and also assuming the temperature independence of the extinction coefficients $\epsilon_{\lambda,LS}$ and $\epsilon_{\lambda,HS}$ for the pure low- and high-spin species respectively. With these assumptions eq 1 was used to calculate extinctions as a function of temperature. The extinctions at 15 different

$$K = \exp\left(\frac{\Delta S°}{R} - \frac{\Delta H°}{R}\frac{1}{T}\right)$$
$$\epsilon_\lambda = \epsilon_{LS,\lambda}\frac{1}{1+K} + \epsilon_{HS,\lambda}\frac{K}{1+K} \qquad (1)$$

wavelengths between 367 and 451 nm, $\epsilon_\lambda(T)$, were used to fit $\Delta H°$ and $\Delta S°$ and $\epsilon_{\lambda,LS}$ and $\epsilon_{\lambda,HS}$ for the 15 wavelengths. The function minimized was the sum given in (2). N_λ and N_T are

$$\frac{1}{N_\lambda}\sum_\lambda \frac{1}{N_T}\sum_T (\epsilon_\lambda^{exp}(T) - \epsilon_\lambda^{calc}(T, \Delta H°, \Delta S°, \epsilon_{\lambda,LS}, \epsilon_{\lambda,HS}))^2 \qquad (2)$$

the number of different wavelengths and temperatures respectively. The results for $\epsilon_{\lambda,LS}$ and $\epsilon_{\lambda,HS}$ are displayed in Figure 3, together with the calculated spectra (full lines) and the measured extinctions (different symbols).

The resultant thermodynamic parameters are $\Delta H° = 19.4 \pm 1.0$ kJ mol^{-1}, $\Delta S° = 85 \pm 5$ J mol^{-1} K^{-1}, and $T_c = 228$ K, the quoted uncertainties being based upon the goodness of fit indicated[20] in Figure 3. The low- and high-spin extinction coefficients, ϵ_{LS} and ϵ_{HS}, show maxima at 432 nm (8500) and around 365 nm (930), respectively, which are in the normal range found for MLCT bands of low- and high-spin Fe(II) complexes with this type of ligand.[12]

Magnetic Susceptibility. The magnetic susceptibility of the perchlorate salt of the complex was measured in the temperature range 4−300 K. The derived moment vs temperature curve shows that the compound undergoes a gradual spin transition between 100 and 250 K, remaining nearly constant at <0.56 μ_B for temperatures below 100 K and leveling out at temperatures above 250 K to a constant value of 5.4 μ_B. No thermal hysteresis was observed. A critical temperature T_c of 196 ± 1 K was calculated from a plot of the high-spin fraction vs temperature. Over the temperature range 152−252 K a good linear relation between ln K_{eq} and $1/T$ was observed. For the thermodynamic parameters reported here, $\Delta H° = 18 \pm 1$ kJ mol^{-1} and $\Delta S° = 95 \pm 5$ J mol^{-1} K^{-1},the errors quoted reflect the sensitivity of the derived values chosen for the limiting moments of pure low- and high-spin species.[21] Although the thermodynamic parameters are somewhat different from those determined spectrophotometrically for propionitrile solutions, consideration of the error limits for the two sets of data suggests that detailed discussion of the origin of the differences is unwarranted at present. The low-spin state of the present compound is stabilized in solution, T_c increasing by 32 K compared to the solid state value. The reason evidently lies with the cooperative interactions that exist in the solid and which reduce the energy difference between the lowest vibronic levels of the high- and low-spin states.[22]

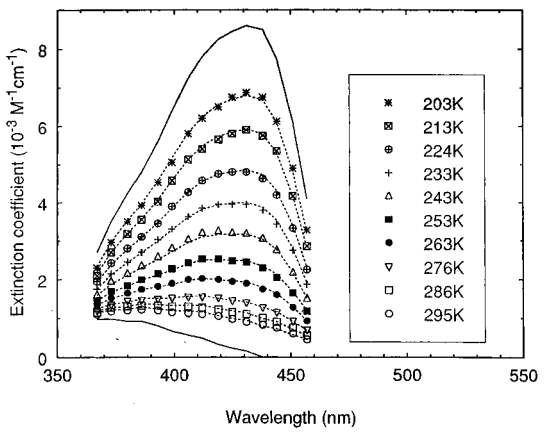

Figure 3. Measured extinction coefficients at temperatures between 203 and 295 K in propionitrile at 15 different wavelengths in the MLCT band region (marked with different symbols according to temperature). The full lines are drawn through the calculated high-spin and low-spin extinction coefficients, for the thermodynamic parameters $\Delta H° = 19.4$ kJ mol^{-1} and $\Delta S° = 85$ JK^{-1} mol^{-1}, and the dashed lines are drawn between the calculated extinction coefficients at the various temperatures. See text for details.

Relaxation Kinetics. At sample temperatures below *ca.* −25 °C. pulsed irradiation at 355 nm resulted in depletion of the ground state absorbance (Figure 4), monitored over the wavelength range 430−500 nm, followed by an exponential return to the original level.

At temperatures higher than −25 °C only laser scatter was observed. The lowest attainable temperatures were set by solvent freezing points. With the solvent mixture propionitrile + *n*-butyronitrile (4:5 v/v), relaxation measurements were possible down to 170 K. Over the full temperature range investigated the traces remained accurately exponential, with

(16) tp(10)aneN$_3$ is *N*,*N*′,*N*″tris(2-pyridylmethyl)-1,4,7-triazacyclodecane.
(17) Jensen, K. B.; Oshio, H.; Toftlund, H. Manuscript in preparation.
(18) Robinson, M. A.; Curry, J. D.; Busch, D. H., *Inorg. Chem.* **1963**, *37*, 1178.
(19) Jørgensen, C. K., *Acta Chem. Scand.* **1955**, *9*, 1362.
(20) A Van't Hoff plot based on the band areas for the best-fit band profiles and a figure showing observed and calculated band areas are deposited as Supporting Information. While the fits are excellent, it must be pointed out that the thermodynamic parameters $\Delta H°$ and $\Delta S°$ are very sensitive to variations of the intensities of the limiting spectra of high- and low-spin forms. Taking this factor into account, the uncertainties in the derived values of $\Delta H°$ and $\Delta S°$ should be more conservatively quoted as being in the region of ±10%.
(21) Using limiting moments of 0.5 μ_B and 5.47 μ_B for pure low- and high-spin compounds, respectively, yields the thermodyanamic parameters $\Delta H° = 19.9 \pm 0.4$ kJ mol^{-1} and $\Delta S° = 102 \pm 2$ J K^{-1} mol^{-1}, where the errors quoted are standard deviations from the least squares fit between ln K_{eq} and $1/T$. However, in view of the sensitivity of both $\Delta H°$ and $\Delta S°$ to the chosen values for the limiting high- and low-spin magnetic moments, it is appropriate to use more conservative error limits for the derived values, as has been done in the main text. Measured and calculated moments and a least-squares fit are available as Supporting Information.
(22) A reviewer's comment.

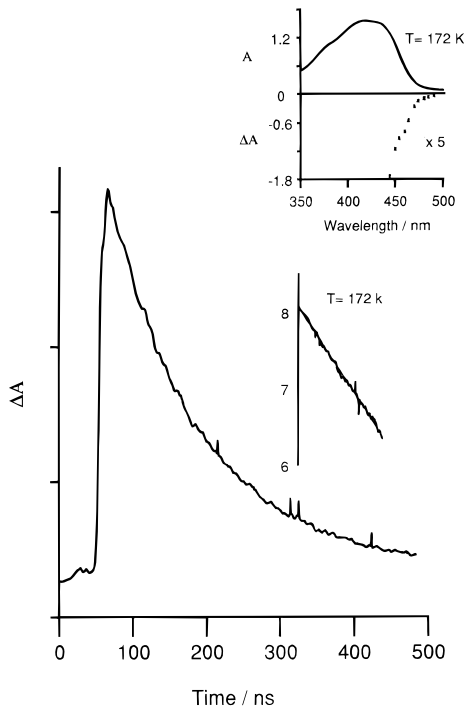

Figure 4. Relaxation trace recorded at 172 K following pulsed laser irradiation of [Fe(tptMetame)]$(ClO_4)_2$ in proprionitrile:butyronitrile (4:5 v/v) at 355 nm, monitored at 460 nm. Goodness of fit is indicated alongside. Upper inset: ground state absorption spectrum and observed pulsed laser-induced depletion as a function of monitoring wavelength.

no indications of biphasic decay (Figure 4). From the measured relaxation times, $\tau = 1/(k_{LS} + k_{HS})$, at various temperatures (τ ranged from 20 to 175 ns over the temperature interval 227−170 K) and the equilibrium constants calculated at these temperatures using the thermodynamic parameters $\Delta H°$ and $\Delta S°$ determined as described above, the individual rate constants for spin crossover, k_{LS} and k_{HS}, were derived. Eyring plots, (ln k)/T vs 1/T, were used to determine the activation parameters: $\Delta H^{‡}_{15} = 25 \pm 2$ kJ mol^{-1}; $\Delta H^{‡}_{51} = 6 \pm 1$ kJ mol^{-1}; $\Delta S^{‡}_{15} = 12 \pm 2$ J K^{-1} mol^{-1}; $\Delta S^{‡}_{51} = -75 \pm 12$ J K^{-1} mol^{-1}. These values are approximate since the thermodynamic parameters used in the evaluation are those derived from spectral measurements in propionitrile and not the propionitrile + butyronitrile solvent mixture used for the relaxation measurements. For the quintet → singlet crossover the activation enthalpy, ≈6 kJ mol^{-1}, (≡500 cm^{-1}) is in the low end of the range frequently reported.[1,23] The activation entropies are calculated on the assumption that the transmission coefficient κ in the Eyring equation

$$k = \kappa(k_B T/h) \exp(\Delta S^{‡}/R) \exp(-\Delta H^{‡}/RT) \qquad (3)$$

is unity i.e. that the HS → LS relaxation process is adiabatic. While this assumption has frequently been questioned, it has been remarked[24] that ascribing the activation entropy completely to nonadiabaticity, corresponding to a lower limit for $\kappa \sim 10^{-4}$, may also not be entirely warranted. On the basis of activation volume measurements[23,25] on other Fe(II) spin crossover systems, it has been suggested[24] that the transition state for spin crossover might be located approximately halfway between the low- and high-spin states, in which case a significantly higher value for the transmission coefficient, $10^{-2} < \kappa < 1$, may be more reasonable. In the present work, the Eyring plots indicate that the spin relaxation process remains thermally activated down to the lowest temperatures investigated (*ca*. 170 K), with no indication of the leveling out that points to low temperature tunneling.[1] Recent studies[1,26] suggest that temperature-independent tunnelling may only be observable at temperatures ≤150 K, conditions which cannot easily be attained in fluid solvent media.[27] However the measured activation enthalpy for the quintet → singlet crossover, *ca*. 500 cm^{-1}, is significantly less than the classical activation barrier that can be estimated[28] on the assumption that the spin crossover takes place along the totally symmetric Fe−N normal coordinate. It has been suggested[28] that the low activation barriers which have now been observed experimentally in several spin crossover systems[1,23,28] can be interpreted as being due to a thermally activated spin relaxation process but one which is nonadiabatic to some degree, involving tunneling from excited vibrational levels of the quintet state, according to the theoretical treatment due to Jortner.[29] On the basis of the data reported here, we should not exclude the possibility that a torsional mode[30] may also contribute to the reaction coordinate for spin crossover, as has previously been suggested elsewhere,[4,23] possibly resulting in a lower activation barrier than would be expected on the basis of a purely radial coordinate.

Computations. Computations were carried out on structures having *R* chirality of the amine nitrogen donors.

Figure 5a,b shows geometry-optimized structures of the diastereomers $\Lambda\lambda^{CAP}$ and $\Lambda\delta^{CAP}$ as calculated by MM with input Fe−N distances of 2.09 and 1.99 Å for sp^3- and sp^2-hybridized nitrogen donors respectively, in accordance with the X-ray data.

MM was used also to optimize the geometry of both the $\Lambda\lambda^{CAP}$ and $\Lambda\delta^{CAP}$ diastereomers for 12 fixed Fe−N distances in the range 1.95−2.7 Å, chosen to span the expected range of distances for the LS and HS isomers. For these calculations the Fe−py distance was kept at a ratio of 0.98 of the Fe−amine distance. For the $\Lambda\delta^{CAP}$ diastereomer with a Fe−N distance of 2.09 Å, the conformations of the pyridyl methyl chelates are not defined as either δ or λ since the C−C vectors are parallel (||) to the N−N vectors. For this $\Lambda\delta^{CAP}$|| || || isomer, when the Fe−N distance exceeds *ca* 2.5 Å the absolute configuration becomes undefined, as the amine−pyridine donor vectors are now parallel to the molecular C_3 axis. However at this core size the conformation of the pyridyl methyl chelates becomes the same as the conformation of the cap, *i.e.* $\delta\delta\delta$. It is possible to trap the molecule in this trigonal prismatic configuration (||$\delta^{CAP}\delta\delta\delta$) and to optimize the structure for the same range of Fe−N distances as used for the above diastereomers. The structure is shown in Figure 5c for an Fe−N distance of 2.1 Å. At the optimized geometry for the three diastereomers, at each of the Fe−N distances, a single point energy calculation was carried out for the ligand alone. While the absolute magnitudes of these energies have no fundamental significance in themselves, comparison of the values for the different diastereomers is instructive. A plot of this energy, $E_{\text{single point}}$, against the Fe−N

(23) (a) McGarvey, J. J.; Lawthers, I.; Heremans, K.; Toftlund, H. *J. Chem. Soc., Chem. Commun.* **1984**, 1575; (b) McGarvey, J. J.; Lawthers, I.; Heremans, K.; Toftlund, H. *Inorg. Chem.* **1990,** *29*, 252.
(24) Beattie, J. K. *Adv. Inorg. Chem.* **1988**, *32*, 1.
(25) DiBenedetto, J.; Arkle, V.; Goodwin, H. A.; Ford, P. C. *Inorg. Chem.* **1985**, *24*, 455.
(26) Schenker, S.; Hauser, A. *J. Am. Chem. Soc.* **1994**, *116*, 5497.
(27) Spin relaxation traces recorded for the complex in Nafion 117 membrane as a host matrix displayed clear evidence of thermally-activated behavior over the temperature interval 170−77 K, with relaxation times ranging from 137 ns at 170 K to 3.4 μs at 77 K. This aspect is still being investigated and the findings will be reported elsewhere.
(28) Hauser, A.; Vef, A.; Adler, P. *J. Chem. Phys.* **1991,** *95***,** 8710**.**
(29) Bukhs, E.; Navon, G.; Bixon, M.; Jortner, J. *J. Am. Chem. Soc.* **1980**, *102*, 2918.
(30) Purcell, K. F. *J. Am. Chem. Soc.* **1979**, *101*, 5147.

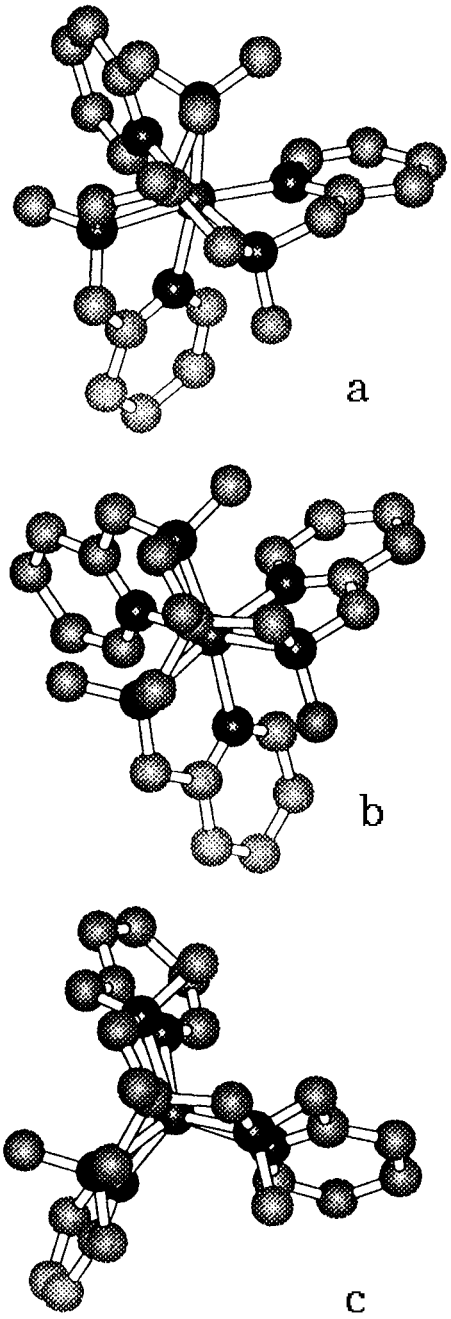

Figure 5. The three diastereomers with lowest internal ligand strain. In each case the enantiomer shown is the one where the nitrogens have R chirality: (a) $\Lambda\lambda^{CAP}\delta\delta\delta$; (b) $\Lambda\delta^{CAP}$ || || ||; (c) $||\delta^{CAP}\delta\delta\delta$.

distance is shown in Figure 6. The calculations indicate that a different core size is preferred by each of the isomers, with the energy minima for the $\Lambda\lambda^{CAP}$, $\Lambda\delta^{CAP}$, and parallel isomers occurring at 2.3, 2.35, and 2.45 Å respectively. It is evident from the plot in Figure 6 that $\Lambda\lambda^{CAP}$ remains the most stable

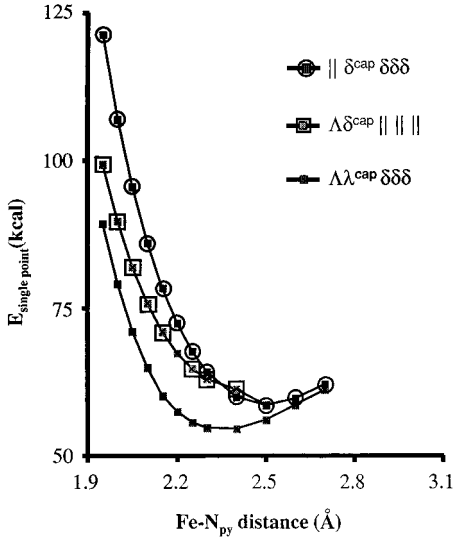

Figure 6. MM+ force field-calculated ligand single point energies for the three diastereomers in Figure 5, plotted against the $Fe-N_{py}$ distance. The $Fe-N_{py}$ distance was kept at 0.98 of the $Fe-N_{amine}$ distance. See text for details.

isomer over the full range of Fe−N distances investigated, indicating that the $\Lambda\lambda^{CAP}$ will be the preferred isomer for both high- and low-spin compounds since the Fe−N distances are always <2.3 Å. The computations are thus consistent with the X-ray data which show that the structure is indeed $\Lambda\lambda^{CAP}\delta\delta\delta$.

The conclusions from the computations are also in accord with the flash photolysis data where single exponential relaxations were observed in all the experiments, over a wide temperature range, pointing to the involvement of one configuration-conformation combination only. This contrasts with the situation we reported in an earlier paper[2] for the $[Fe(tp(10)aneN_3)](ClO_4)_2$ complex where marked biphasic relaxation behavior was observed and attributed to the coupling of ligand configurational or conformational changes to the relaxation process.

Acknowledgment. We thank the EPSRC for support (Grant GR/J01905), the Danish Natural Science Research Council (Grant 11-7916 to K.B.J.) and the EC for a grant under the Human Capital and Mobility Programme (Grant CHRX-CT92-0080).

Supporting Information Available: Figure S1, ORTEP drawing of the $[FetptMetame]^{2+}$ cation, displaying thermal ellipsoids drawn at the 50% probability level. Tables S1 and S2, containing a complete listing of atomic coordinates and isotropic thermal parameters, bond lengths, and bond angles. Figures S2-S6, observed and calculated band integrals of UV−vis spectra in solution, measured and calculated solid state magnetic moments and van't Hoff plots, and Eyring plots of spin crossover relaxation data. (11 pages). Ordering information is given on any current masthead page.

IC960228G